10) Verniory, A., R. Du Bois, P. Decoodt, J. P. Gassee and P. P. Lambert: *J. Gen. Physiol.*, **62**, 489 (1973).
11) Wang, N. H. L. and K. H. Keller: *Trans. Am. Soc. Artif. Intern. Organs*, **25**, 14 (1979).
12) Zydney, A. L. and C. K. Colton: *Trans. Am. Soc. Artif. Intern. Organs*, **28**, 408 (1982).

(Presented in part at the 51st Annual Meeting of The Society of Chemical Engineering, Japan, at Osaka, March 1986.)

STRUCTURAL ANALYSIS OF HOLLOW FIBER DIALYSIS MEMBRANES FOR CLINICAL USE

KIYOTAKA SAKAI, SHINGO TAKESAWA, RISHICHI MIMURA AND HIDEHIKO OHASHI

Department of Chemical Engineering, Waseda University, Tokyo 160

Key Words: Dialysis Membrane, Pore Radius, Solute Permeability, Pure Water Permeability, Surface Porosity, Tortuosity, Water Content

Little is known of the structure of hollow-fiber dialysis membranes for clinical use or of the effects of structure on solute and pure water permeability. Knowledge of such aspects of membrane structure as pore radius, surface porosity, tortuosity and water content is required if the desired membranes are to be designed.

The objective of the present study, therefore, is to obtain data on the pore radius, surface porosity and tortuosity of hollow-fiber dialysis membranes through an analysis of measured water content, and of solute and pure water permeability on the basis of a newly introduced tortuous pore model. In regenerated cellulose membranes, pore radius ranges from 21 to 34×10^{-10} m, and huge pores ranging in radius from 47 to 64×10^{-10} m are identified for EVA membranes which are permeable to small amounts of serum protein. Values for surface porosity of the regenerated cellulose and EVA membranes are approximately 33 and 22%, and tortuosity is approximately 1.9 and 2.2, respectively. The tortuous pore model combined with the L_p and P_m method is well suited for elucidating the relationship between membrane structure and solute and pure water permeability.

Introduction

The performance of currently utilized hemodialyzers is absolutely dependent on the permeability of their membranes. Appropriate design of dialysis membranes requires correct values for pore radius, surface porosity, water content and tortuosity. It has proved impossible to find the pore radius of dialysis membranes using the mercury porosimeter or electron microscope because the pores are only several tens of angstroms in radius. Consequently, indirect procedures such as the L_p method that uses both pure water permeability and water content,[1] the L_p and P_m method, which uses both pure water and solute permeability[4,5,7,8] and the σ method that uses the reflection coefficient[3,8,14] have been employed extensively. Structural data obtained from the procedures referred to above may lack reliability, however, because those procedures depend on a simplified pore model that assumes that membrane pores are formed perpendicular to the membrane surface.

The objective of the present study is to obtain data on the pore radius, surface porosity and tortuosity of hollow-fiber dialysis membranes through an analysis of measured water content, and of solute and pure water permeability on the basis of a newly introduced tortuous pore model.

1. Theoretical

Kedem and Katchalsky[2] derived phenomenological transport equations based on nonequilibrium thermodynamics. In this analysis, membrane characteristics are expressed as three transport parameters—reflection coefficient, and solute and pure water permeability. The membrane is considered to be a black box.

The simplified pore model[7] directly relating membrane structure to these transport parameters was improved by Verniory[13] and Kimura[6] with tortuosity omitted in any pore model. Qualitative attempts to account for tortuosity in the pore model have been successful.[9]

Received October 1, 1986. Correspondence concerning this article should be addressed to K. Sakai.

Tortuosity τ may be defined as the ratio of pore length to wall thickness:

$$\tau = L/\Delta x \tag{1}$$

The pore model was further improved to produce the following equations:

$$L_p = (r_p^2/8\mu)(A_k/\tau/\Delta x) \tag{2}$$

$$P_m = D_W f(q) S_D (A_k/\tau/\Delta x) \tag{3}$$

where

$$f(q) = (1 - 2.105q + 2.0865q^3 - 1.7068q^5 + 0.72603q^6)/(1 - 0.75857q^5) \tag{4}$$

$$S_D = (1-q)^2 \tag{5}$$

$$q = r_s/r_p \tag{6}$$

From Eqs. (2) and (3),

$$P_m/L_p = f(q) S_D (8\mu D_W/r_p^2) \tag{7}$$

which is identical with the equation obtained by Klein.[4)]

Structural parameters such as surface porosity, tortuosity and wall thickness involved in the pore model disappear in Eq. (7). Measurements of solute and pure water permeability provide pore radius by iteration without using surface porosity, water content, tortuosity or wall thickness. Values for $A_k/(\tau \cdot \Delta x)$ can be obtained by substituting pore radius and pure water permeability data in Eq. (2).

The pore length in Eq. (1) cannot be measured in a straightforward way. Water is capable of permeating the amorphous region of the crystalline polymer that forms the pores in dialysis membranes. The water content approximates pore volume ratio under wet conditions. The tortuosity defined in Eq. (1) can be alternatively expressed as

$$\tau = \frac{(nA_pL)/V_m}{(nA_p\Delta x)/V_m} = \frac{(nA_pL)/V_m}{(nA_p)/A_m} = \frac{H}{A_k} \tag{8}$$

Here τ and A_k can be calculated from Eqs. (9) and (10).

$$\tau = \sqrt{H/\Delta x/(A_k/\tau/\Delta x)} \tag{9}$$

$$A_k = \sqrt{H\Delta x(A_k/\tau/\Delta x)} \tag{10}$$

In the tortuous pore model presented here, dialysis membranes are assumed to be of symmetrical structure. With imperfectly symmetrical dialysis membranes, structural parameters obtained by the tortuous pore model are averaged over pore length.

2. Experimental

2.1 Materials

Table 1 summarizes technical data on the capillary dialyzers tested. Hollow-fiber dialysis membranes prepared from polymers such as regenerated cellulose (RC), ethylenevinyl alcohol (EVA) and polymethyl methacrylate (PMMA) are skinfree and of imperfectly symmetrical structure.

Stokes radius and diffusivity at 310 K are as follows:[12]

Urea	$r_s = 1.82 \times 10^{-10}$ m	$D_W = 1.81 \times 10^{-9}$ m$^2 \cdot$s^{-1}
Glucose	$r_s = 3.61 \times 10^{-10}$ m	$D_W = 9.09 \times 10^{-10}$ m$^2 \cdot$s^{-1}
Sucrose	$r_s = 4.71 \times 10^{-10}$ m	$D_W = 6.97 \times 10^{-10}$ m$^2 \cdot$s^{-1}

Water viscosity at 310 K is 6.947×10^{-4} Pa·s.

2.2 Apparatus

The experimental apparatus shown in **Fig. 1** was utilized to measure solute permeability at a dialysate flow rate (**Fig. 2**) sufficient to eliminate the boundary layer formed outside the membrane tube.

2.3 Procedures

The slope of the plot of TMP (transmembrane pressure) vs. ultrafiltration rate provides pure water permeability. Solute permeability was determined by a newly improved method using ^{14}C-labeled urea, glucose and sucrose.

The following procedure was used:

1. The hollow-fiber membranes available from the dialyzers tested were cut into shorter lengths, and the effective length was kept to 0.1 m by equipping each membrane with polyethylene tubes (ID 1 mm; OD 2 mm) at either end.
2. The membranes were placed in pure water at 310 K for 12 h to completely wet them.
3. The hollow was filled with the desired radioactive solute in pure water containing 5Cim^{-3} after water removal and the membrane was sealed with clay. Dialysis experiments were then conducted for a predetermined time.
4. The amount of radioactive solute remaining in the sealed membrane tube was determined, using an Aloka-900LSC liquid scintillation counter.

Five or more measurements were made for various dialysis times to obtain exact values for solute permeability, and data were analyzed by the method of Stevenson.[10,11)] One hundred wet membrane tube sections were observed under a microscope to determine both inner diameter and wall thickness when

Table 1. Technical data on capillary dialyzer

Dialyzer (Manufacturer)	Number of fibers	Material	Surface area [m^2]	Membrane		
				Inner diameter $\times 10^6$ [m]	Wall thickness $\times 10^6$ [m]	Fiber length $\times 10^3$ [m]
MC 0.8H (Senko Med. Co., Ltd.)	6,600	Cuprophan®	0.72	200	8	172
TAF 10 (Terumo Co., Ltd.)	6,850	Regenerated cellulose	1.02	200	12	237
AM-10 (Asahi Med. Co., Ltd.)	10,700	Regenerated cellulose	1.18	200	15	176
AM-2000U (Asahi Med. Co., Ltd.)	10,900	Regenerated cellulose	1.49	200	8	218
KF-101 (Kuraray Co., Ltd.)	7,800	Ethylenevinyl alcohol	1.21	200	32	246
KF-101C (Kuraray Co., Ltd.)	7,800	Ethylenevinyl alcohol	1.23	200	32	250
KPK-101 (Kuraray Co., Ltd.)	6,528	Ethylenevinyl alcohol	1.26	250	33	245
B2-100 (Toray Med. Co., Ltd.)	11,000	Polymethyl methacrylate	1.21	200	25	175

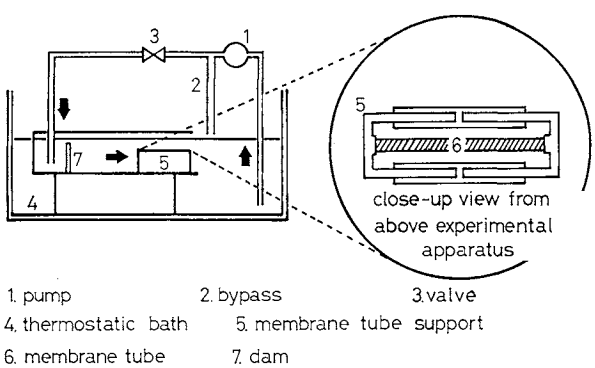

Fig. 1. Experimental apparatus for measuring solute permeability.

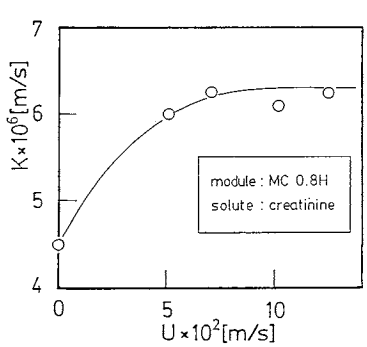

Fig. 2. Effects of dialysate flow rate on overall mass transfer coefficient for creatinine.

wet. Water content was measured by the standard method using 120 membrane tubes 5×10^{-2} m in length.

3. Results

3.1 Inner diameter and wall thickness of wet hollow-fiber dialysis membranes

Table 2 summarizes both the inner diameter and wall thickness of the hollow-fiber dialysis membranes tested under wet conditions. The wet RC membranes swelled two- or threefold in wall thickness. The wet EVA membranes exhibited some increase in wall thickness but almost no alteration in inner diameter because of the resistance to inward expansion.

Table 2. Inner diameter and wall thickness of hollow-fiber dialysis membranes

Dialyzer	Inner diameter* $\times 10^6$ [m]	Wall thickness* $\times 10^6$ [m]
MC 0.8H	212±13	20.7±2.8
TAF 10	203±11	26.4±2.9
AM-10	204±22	30.7±2.4
AM-2000U	200±12	19.2±2.2
KF-101	228±14	41.1±5.2
KF-101C	220±10	44.3±4.2
KPK-101	251±23	51.8±5.2
B2-100	202± 7	25.3±2.4

* Data taken under wet conditions and expressed in mean±S.D.; N=100.

3.2 Solute permeability

Table 3 summarizes the measured values for solute permeability of the membranes tested. The solute permeability of the RC membranes was highly dependent on wall thickness. Because of their greater thickness, synthetic polymer membranes are permeated more slowly than RC membranes by substances of small molecular weight. The EVA membranes permeable to small amounts of serum albumin appear to have huge pores, and middle molecules (MM) may adequately permeate them.

Table 3. Water content, solute and pure water permeability data of hollow-fiber dialysis membranes

Dialyzer	Solute permeability $\times 10^6$ [m·s^{-1}]*			Pure water permeability $L_p \times 10^{11}$ [m^3·m^{-2}·s^{-1}·Pa^{-1}]**	Water content H [v/v %]***
	Urea (62)	Glucose (180)	Sucrose (342)		
MC 0.8H	11.6 ±3.7 (20)	4.79±0.35 (12)	2.66±0.19 (15)	1.11	66
TAF 10	8.42±0.23 (4)	2.83±0.06 (4)	2.16±0.05 (4)	1.12	61
AM-10	7.83±0.13 (15)	3.08±0.09 (10)	1.80±0.10 (10)	0.588	65
AM-2000U	12.2 ±1.1 (5)	5.15±0.12 (6)	3.06±0.07 (5)	1.58	61
KF-101	3.52±0.17 (11)	1.83±0.08 (10)	0.91±0.05 (10)	0.936	46
KF-101C	4.02±0.08 (10)	1.81±0.03 (8)	1.08±0.03 (8)	1.64	49
KPK-101	5.23±0.29 (7)	2.41±0.04 (4)	1.42±0.04 (4)	2.31	nil
B2-100	*6.51* (1)	2.94 (1)	2.11 (1)	0.638	54

* Data expressed in mean±S.D. (N).
** Data measured at 310 K.
*** Data measured at room temperature.

3.3 Pure water permeability

Pure water permeability increases significantly with pore radius. Measured values for pure water permeability in Table 3 indicate the presence of an appreciable number of huge pores on such EVA membranes as KF-101C and KPK-101. Among the RC membranes, AM-2000U provided the highest pure water permeability. KPK-101, with greater thickness than KF-101C, possessed higher pure water permeability.

3.4 Water content

Water content is easily measurable and provides a reliable parameter for controlling the permeability of dialysis membranes, and permeability is directly proportional to water content for a specified membrane. However, water content merely represents the volume fraction of pores in the membranes, and cannot be used to find the permeability of different kinds of dialysis membranes. It is thus necessary to know pore radius, surface porosity and tortuosity as well as water content to reveal the structure of a membrane and the effects of structure on solute and pure water permeability.

4. Discussion

4.1 Solute permeability

Figure 3 shows the dependence of solute permeability on the Stokes radius of the solutes tested for typical membranes of regenerated cellulose (MC0.8H and TAF10) and synthetic polymer (KF-101). All membranes showed linear relationships. The RC membranes possessed the highest permeability for substances with a molecular weight of below 500 daltons, mainly because of their lesser thickness. The difference in solute permeability between MC0.8H and TAF10 can be also explained in terms of wall thickness.

4.2 P_m/L_p and r_p (L_p and P_m method)

According to the tortuous pore model, P_m/L_p is a function of both Stokes radius r_s and pore radius r_p. Since P_m/L_p is expressed as a polynomial of r_p for a specified solute, several values for pore radius can be obtained. The measured value of P_m/L_p usually provides two values for pore radius. A theoretically appropriate pore radius was determined by excluding other values with an abnormally high surface porosity.

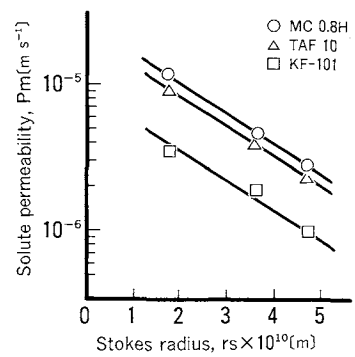

Fig. 3. Dependence of solute permeability on Stokes radius for MC0.8H, TAF10 and KF-101.

4.3 r_{p1}, A_k and τ

Table 4 summarizes values for pore radius r_{p1} iteratively calculated using Eq. (7) for hollow-fiber dialysis membranes. Pore radius r_{p1} is a mean value because dialysis membranes usually have a pore radius distribution and are of imperfectly symmetrical structure. All membranes had practically the same pore radius for the three solutes tested.

The tortuosity of membrane pores is defined in Eq. (1) and was calculated by Eq. (9). Surface porosity was also calculated by Eq. (10). Calculated values for τ and A_k are summarized in Table 4. A higher tortuosity implies a convoluted passage for solute transport, causing reduced solute and pure water permeability. The synthetic polymer membranes possess a higher tortuosity. Surface porosity affecting solute and pure water permeability is lowered in synthetic

Table 4. Calculation of r_{p1}, $A_k/(\tau \cdot \Delta x)$, A_k and τ by L_p and P_m method

Dialyzer	$r_{p1} \times 10^{10}$ [m]				$A_k/(\tau \cdot \Delta x) \times 10^{-3}$ [m^{-1}]				A_k [%]	τ [—]
	Urea	Glucose	Sucrose	Mean	Urea	Glucose	Sucrose	Mean		
MC 0.8H	26.6	24.4	26.0	25.7	8.62	10.4	9.02	9.35	34	1.9
TAF-10	32.3	36.0	32.1	33.5	5.91	4.85	6.10	5.62	31	2.0
AM-10	23.0	20.6	19.7	21.1	6.12	7.75	8.50	7.46	35	1.9
AM-2000U	31.8	30.2	32.0	31.3	8.59	9.64	8.33	8.85	32	1.9
KF-101	47.5	42.3	51.4	47.1	2.29	2.92	1.95	2.39	21	2.2
KF-101C	60.3	60.1	66.5	62.3	2.53	2.57	2.10	2.40	23	2.1
KPK-101	62.5	61.6	68.8	64.3	3.26	3.42	2.74	3.14	nil	nil
B2-100	26.8	nil	nil	26.8	4.84	nil	nil	4.84	25	2.2

polymer membranes. The surface porosity and water content of AM-10 and MC0.8H are higher than those of the other RC membranes.

4.4 Pore radius r_{p2} based on the L_p method

To determine pore radius r_{p2} by the L_p method, we need pure water permeability, water content and wall thickness but not tortuosity. Eq. (11) provides pore radius r_{p2} for the membranes tested:

$$L_p = (r_{p2}^2/8\mu)(H/\Delta x) \qquad (11)$$

Table 5 shows values for pore radius r_{p2}, and all values are lower than those for pore radius r_{p1} obtained from Eq. (7). KF-101 membrane possesses a much smaller pore radius r_{p2} than the Stokes radius r_s of serum albumin, and this does not accord with the fact that KF-101 membrane is permeable to serum albumin to some extent.

4.5 Pore radius r_{p3} based on the P_m method

Using the P_m method, pore radius r_{p3} can be calculated from solute permeability, water content and wall thickness; again tortuosity is not needed.

$$P_m = D_W f(q) S_D (H/\Delta x) \qquad (12)$$

Table 5 summarizes values for r_{p3} calculated by Eq. (12). The values for r_{p3} are even lower than those for r_{p2}. With Nuclepore membranes, pore radius r_{p2} and r_{p3} appear to be almost the same as r_{p1} because the tortuosity is close to unity.

Table 5. Calculation of pore radii r_{p2} and r_{p3} by L_p method and P_m method

Dialyzer	$r_{p2} \times 10^{10}$ [m]	$r_{p3} \times 10^{10}$ [m]		
		Urea	Glucose	Sucrose
MC 0.8H	13.9	6.0	10.8	12.5
TAF 10	16.4	6.0	10.0	13.0
AM-10	12.4	6.0	10.7	12.6
AM-2000U	16.7	6.2	11.3	13.2
KF-101	21.5	5.4	11.3	12.4
KF-101C	28.6	5.9	11.3	13.2
B2-100	12.8	5.5	10.5	13.3

Conclusions

1. It was found that RC membranes had a mean pore radius from 21 to 34×10^{-10} m, a surface porosity from 31 to 35% and a tortuosity from 1.9 to 2.0.
2. EVA membranes possess higher values for pore radius and tortuosity than RC membranes.
3. The tortuous pore model combined with the L_p and P_m method is especially useful in the structural analysis of hollow-fiber membranes for clinical dialysis applications.

Acknowledgment

The authors are indebted to Mr. S. Yamane at Tokyo Tokatsu Clinic, Chiba, Japan for help and advice with the analytical procedures of radioisotope-labeled solutes, and to Miss R. Yamamoto for typing the manuscript.

Nomenclature

A_k	=	fractional surface porosity	[—]
A_m	=	membrane area	[m^2]
A_p	=	sectional area of pore	[m^2]
D_W	=	diffusivity	[m$^2 \cdot$s^{-1}]
$f(q)$	=	wall correction factor for diffusion	[—]
H	=	fractional water content	[—]
K	=	overall mass transfer coefficient	[m$\cdot$s^{-1}]
L	=	pore length	[m]
L_p	=	pure water permeability	[m$^3 \cdot$m$^2 \cdot$s$^{-1} \cdot$Pa^{-1}]
n	=	number of pores	[—]
P_m	=	solute permeability	[m$\cdot$s^{-1}]
q	=	r_s/r_p	[—]
r_p	=	radius of membrane pore	[m]
r_{p1}	=	pore radius calculated by Eq. (7)	[m]
r_{p2}	=	pore radius calculated by Eq. (11)	[m]
r_{p3}	=	pore radius calculated by Eq. (12)	[m]
r_s	=	Stokes radius of solute	[m]
S_D	=	steric hindrance factor for diffusion	[—]
U	=	dialysate flow rate	[m$\cdot$s^{-1}]
V_m	=	membrane volume	[m^3]
Δx	=	Wall thickness	[m]
μ	=	viscosity	[Pa$\cdot$s]
τ	=	tortuosity	[—]

Literature Cited

1) Ferry, J. D.: *Chem. Rev.*, **18**, 373 (1936).
2) Kedem, O. and A. Katchalsky: *Biochim. Biophys. Acta*, **27**, 229 (1985).

3) Klein, E., F. F. Holland and K. Eberle: *asaio J.* **1**, 15 (1978).
4) Klein, E., F. F. Holland and K. Eberle: *J. Membrane Sci.*, **5**, 173 (1979).
5) Madras, S., R. L. McIntosh and S. G. Mason: *Can. J. Res.*, **B27**, 764 (1949).
6) Nakao, S. and S. Kimura: *J. Chem. Eng. Japan*, **15**, 220 (1982).
7) Pappenheimer, J. R., E. M. Renkin and L. M. Borrero: *Am. J. Physiol.*, **167**, 13 (1951).
8) Renkin, E. M.: *J. Gen. Physiol.*, **38**, 225 (1954).
9) Sakai, Y. and H. Tanzawa: *J. Appl. Polym. Sci.*, **22**, 1805 (1978).
10) Stevenson, J. F.: *Am. Inst. Chem. Eng. J.*, **20**, 461 (1974).
11) Stevenson, J. F., M. A. Von Deak, M. Weinberg and R. W. Schuette: *Am. Inst. Chem. Eng. J.*, **21**, 1192 (1975).
12) Takesawa, S., K. Ozawa, R. Mimura and K. Sakai: *Japan. J. Artif. Organs*, **13**, 1460 (1984).
13) Verniory, A., R. Dubois, P. Decoodt, J. P. Gassee and P. P. Lambert: *J. Gen. Physiol.*, **62**, 489 (1973).
14) Wendt, R. P., E. Klein, E. H. Bresler, F. F. Holland, R. M. Serino and H. Villa: *J. Membrane Sci.*, **5**, 23 (1979).

(Presented in part at the 49th Annual Meeting of The Society of Chemical Engineers of Japan, Nagoya, April 1984.)

ON SECOND VIRIAL COEFFICIENTS OF GASES AND GAS MIXTURES

YUJI TANAKA AND DABIR S. VISWANATH
Department of Chemical Engineering, University of Missouri-Columbia, Columbia, Missouri 65211, U.S.A.

Key Words: Gas, Gas Mixture, Virial Equation, Second Virial Coefficient, Third Parameter

Molar refraction and molar polarization were used as new third parameters to correlate the second virial coefficients of nonpolar and polar gases, and their mixtures. A set of consistent data from the compilation of Dymond and Smith[6] was used for the source data. The correlation was compared extensively with the correlations of Tsonopoulos, Tarakad-Danner, Brewer, Kubic and Vetere. In addition to the new third parameter, the utility of Pitzer's acentric factor was also tested. The correlation developed was of the general type

$$BPc/RTc = f^{(0)}(T/Tc) + \kappa \cdot f^{(1)}(T/Tc) \qquad (1)$$

Where κ is the third parameter.

Introduction

The non-ideal behavior of gases arising from intermolecular interactions in principle can be explained through the virial coefficients. The virial coefficients, either in pressure or reciprocal volume series, can be evaluated using potential energy functions such as the Lennard-Jones potential energy function.

The virial equation

$$Z = 1 + B'P + C'P^2 + \text{higher-order terms} \qquad (2)$$

or

$$Z = 1 + B/V + C/V^2 + \text{higher-order terms} \qquad (3)$$

is often truncated after the second term. There are several reasons for the use of B only. For example, (i) experimental virial coefficients other than B are rarely available, and even if available are of very low accuracy; (ii) when the virial equation is used for moderate pressures, it is sufficient to use the second virial coefficients; (iii) the virial equation by its nature diverges at higher density and therefore its application is limited in spite of the theoretical background; and (iv) virial coefficients higher than the third with the non-additive contribution have not been evaluated for potential energy functions other than the Lennard-Jones potential function.

Pitzer[14] did the first work on the generalization of second virial coefficients by introducing a third parameter, the acentric factor, ω. Its applicability is limited to nonpolar and slightly polar compounds only. Also, experimental data of the vapor pressure at $Tr = 0.7$ is needed. Tsonopoulos[18] modified Pitzer's equation for polar compounds. This correlation with nine to eleven constants can predict the second virial

Received October 3, 1986. Correspondence concerning this article should be addressed to D. S. Viswanath.